Cellular/Molecular

KCNQ/M Currents in Sensory Neurons: Significance for Pain Therapy

Gayle M. Passmore,[1] Alexander A. Selyanko,[1]† Mohini Mistry,[1] Mona Al-Qatari,[1] Stephen J. Marsh,[1] Elizabeth A. Matthews,[1] Anthony H. Dickenson,[1] Terry A. Brown,[2] Stephen A. Burbidge,[2] Martin Main,[3] and David A. Brown[1]

[1]Department of Pharmacology, University College London, London WC1E 6BT, United Kingdom, [2]Neurological and Gastrointestinal Diseases Centre of Excellence for Drug Discovery, GlaxoSmithKline, Harlow CM19 5AW, United Kingdom, and [3]Systems Research, GlaxoSmithKline, Medicines Research Centre, Stevenage SG1 2NY, United Kingdom

Neuronal hyperexcitability is a feature of epilepsy and both inflammatory and neuropathic pain. M currents [$I_{K(M)}$] play a key role in regulating neuronal excitability, and mutations in neuronal KCNQ2/3 subunits, the molecular correlates of $I_{K(M)}$, have previously been linked to benign familial neonatal epilepsy. Here, we demonstrate that KCNQ/M channels are also present in nociceptive sensory systems. $I_{K(M)}$ was identified, on the basis of biophysical and pharmacological properties, in cultured neurons isolated from dorsal root ganglia (DRGs) from 17-d-old rats. Currents were inhibited by the M-channel blockers linopirdine (IC$_{50}$, 2.1 μM) and XE991 (IC$_{50}$, 0.26 μM) and enhanced by retigabine (10 μM). The expression of neuronal KCNQ subunits in DRG neurons was confirmed using reverse transcription-PCR and single-cell PCR analysis and by immunofluorescence. Retigabine, applied to the dorsal spinal cord, inhibited C and Aδ fiber-mediated responses of dorsal horn neurons evoked by natural or electrical afferent stimulation and the progressive "windup" discharge with repetitive stimulation in normal rats and in rats subjected to spinal nerve ligation. Retigabine also inhibited responses to intrapaw application of carrageenan in a rat model of chronic pain; this was reversed by XE991. It is suggested that $I_{K(M)}$ plays a key role in controlling the excitability of nociceptors and may represent a novel analgesic target.

Key words: M-current; dorsal root ganglion; neuropathic pain; retigabine; KCNQ; nociceptors

Introduction

Pain can arise from tissue and nerve damage. The former is generally well controlled, whereas neuropathic pain is not. Neuropathic pain, defined as "pain initiated or caused by a primary lesion or dysfunction in the nervous system" (Suzuki and Dickenson, 2000), is characterized by sensations such as deep aching, increased sensitivity to noxious stimuli (hyperalgesia), and the perception of pain in response to innocuous stimuli (allodynia). It is conveyed from the periphery to the CNS by way of primary afferent neurons known as nociceptors, which respond to noxious mechanical, thermal, and chemical stimuli. Although growing numbers of pharmacological agents for the treatment of neuropathic pain are readily available (several of which were originally used as anticonvulsants), effective pain control without side effects has yet to be fully achieved (for review, see Hunt and Mantyh, 2001; Jensen et al., 2001). Furthermore, neuropathic

pain can be refractory to analgesics such as morphine (Suzuki et al., 2002).

A feature of neuropathic pain is neuronal hyperexcitability. K$^+$ channels play an essential role in setting the resting membrane potential and in controlling the excitability of neurons. The opening of K$^+$ channels leads to hyperpolarization of the cell membrane, which results in a decrease in cell excitability. Thus, K$^+$ channels represent potentially attractive peripheral targets for the treatment of pain. Although many studies have focused on the role of Na$^+$ channels in pain, few have considered the role of K$^+$ channels (for review, see McCleskey and Gold, 1999; Waxman et al., 1999) (Ishikawa et al., 1999; Boettger et al., 2002).

One K$^+$ channel that is known to regulate excitability in a variety of central and peripheral neurons is the M channel (K$_M$; Brown, 1988; Marrion, 1997). Thus, mutations of its constituent KCNQ2 or KCNQ3 subunits (Wang et al., 1998) have been genetically linked to a form of epilepsy known as benign familial neonatal convulsions (Jentsch, 2000), whereas deletion of one KCNQ2 allele in mice enhances sensitivity to epileptogenic agents (Watanabe et al., 2000), both manifestations of disordered excitability. The presence of M currents [$I_{K(M)}$] in sensory neurons has previously been reported in bullfrog dorsal root ganglia (Tokimasa and Akasu, 1990) but not hitherto in mammalian ganglia. However, the finding that the anticonvulsant drug retigabine can alleviate some forms of chronic pain (A. Rostock, C. Rundfeldt, and R. Bartsch, presentation to the Deutschen Gesell-

schaft für Pharmakologie und Toxikologie, 2000; Blackburn-Munro and Jensen, 2003) implies that M channels might regulate nociceptive sensory neuron activity, because retigabine enhances the activity of KCNQ2/3 channels (Main et al., 2000; Rundfeldt and Netzer, 2000; Wickenden et al., 2000; Tatulian et al., 2001).

In this work, we have identified functional M channels and their constituent molecular KCNQ subunits in sensory neurons from rat dorsal root ganglia. We then show that retigabine enhances currents through these channels and reduces both electrophysiological and behavioral manifestations of enhanced nociceptive activity in experimental models of persistent pain. These results imply that $I_{K(M)}$ plays a key role in regulating excitability in nociceptors and may therefore present a novel therapeutic target for the treatment of pain.

Parts of this manuscript have been published previously in abstract form (Selyanko et al., 2001).

Materials and Methods
Cell culture
Dorsal root ganglion and superior cervical ganglion neurons. Dorsal root ganglion (DRG, from all spinal levels) and superior cervical ganglion (SCG) neurons were dissected from 17-d-old Sprague Dawley rats killed by CO_2 asphyxiation and prepared using a standard enzymatic dissociation procedure as described elsewhere (Owen et al., 1990). Briefly, after incubation in collagenase (500 U/ml for 15 min) and then trypsin (1 mg/ml for 30 min), the ganglia were mechanically triturated with a fire-polished glass Pasteur pipette. The ganglia were then centrifuged and resuspended in Leibovitz' L-15 supplemented with 10% fetal calf serum (FCS), 2 mM glutamine, 24 mM $NaHCO_3$, 38 mM glucose, 2-3% penicillin and streptomycin, and 25 ng/ml nerve growth factor. For electrophysiological recording, dissociated neurons were plated on 35 mm plastic dishes (Nunc, Roskilde, Denmark) coated with laminin and used either 1–2 (SCG) or 1–8 (DRG) d in culture. For immunofluorescence, dissociated DRG neurons were plated onto laminin-coated glass coverslips contained within four-well sterile tissue culture plates and used 1 d in culture.

Chinese hamster ovary cells. Chinese hamster ovary (CHO) cells were cultured and transfected as described elsewhere (Selyanko et al., 1999). Briefly, CHO cells were grown at 37°C and 5% CO_2 in α-MEM supplemented with 10% FCS, 1% L-glutamine, and 1% penicillin and streptomycin. Cells were plated in 35 mm plastic dishes and transfected 1 d later using LipofectAMINE Plus according to the manufacturer's instructions (Invitrogen, San Diego, CA). KCNQ and CD8 cDNA plasmids, driven by the cytomegalovirus promoter, were cotransfected in a 10:1 ratio. For expression of heteromultimers, equal amounts of human KCNQ2 and rat KCNQ3 cDNAs were used (obtained from Dr. D. McKinnon, State University of New York, Stony Brook, NY), as described by Wang et al. (1998). Transfected cells were identified by adding CD8-binding Dynabeads (Dynal, Oslo, Norway) before recording.

Perforated patch whole-cell recording
Solutions. The extracellular solution contained (in mM): 144 NaCl, 2.5 KCl, 2 $CaCl_2$, 0.5 $MgCl_2$, 5 HEPES, and 10 glucose, pH adjusted to 7.4 with Tris base. Pipettes were filled with an intracellular solution containing (in mM): 80 K acetate, 30 KCl, 40 HEPES, 3 $MgCl_2$, 3 EGTA, and 1 $CaCl_2$, pH adjusted to 7.4 with NaOH. Amphotericin B was used to perforate the patch (Rae et al., 1991). Pipette resistance was 2–3 MΩ, and the series resistance was compensated (60–90%). Recordings were made at room temperature (20–22°C).

Data acquisition and analysis. Data were acquired and analyzed using pClamp software (version 8.0; Axon Instruments). Currents were recorded using an Axopatch 200A (or 200B) patch-clamp amplifier, filtered at 1 kHz, and digitized at 4–8 kHz. $I_{K(M)}$ amplitude and its inhibition by K^+ channel blockers were measured from deactivation relaxations at −50 mV. Results are expressed as mean ± SEM. In general, half-inhibitions were calculated using the Hill equation: $y/y_{max} = 1/(1 + (x/x_0)^p)$, where y is the fractional reduction of the relaxation amplitude; y_{max} is the maximum reduction; x is the drug/blocker concentration; x_0 is

the IC_{50} (the concentration at which $y/y_{max} = 0.5$), and p is the power (equivalent to the Hill slope). However, for tetraethylammonium (TEA) sensitivity, some of the inhibition curves were best fit using a two-component equation: $y/y_{max} = q/(1 + x/x_0) + (1 - q)/(1 + x/x_1)$, where x_0 and x_1 are the IC_{50} values for two channel populations with proportional contributions of q and $(1 - q)$, respectively (other definitions are as above). The program Origin (version 5.0; Microcal Software Inc.) was used for creating the figures.

PCR analyses
Reverse transcription-PCR. Sequence-specific oligonucleotide primers were designed to the 3′ coding and or noncoding regions of all members of the KCNQ gene family. Alignments of rat, where available, or human KCNQ cDNA sequences allowed the design of KCNQ subtype-specific primers. The primer sequences were as follows: KCNQ1, forward, AGGATCGGAGGCCAGACCAT; reverse, TCATATCAGGCCTTCAA-GAG; KCNQ2, forward, AAGCTAGACTTCCTGGTGAG; reverse, ACTGTATGTGCTAAGGAACC; KCNQ3, forward, AAGACAGGT-TCACGACATGG; reverse, CTAGAAGAGACTAACAGTGC; KCNQ4, forward, GCCGGATCAAGAGCCTGCAA; reverse, CCAAGCAGCCT-GAGACCAGCT; and KCNQ5, forward, CTGTCATTCGAGCTAT-CAGA; reverse, GCTTGACTGTGCATAGTAGG.

Rat DRG total RNA was purified from whole DRG by homogenization in Trizol reagent (Invitrogen, Paisley, UK) according to the manufacturer's instructions. Rat total RNA samples from heart and skeletal muscle were obtained from Clontech (Palo Alto, CA). Total RNA was reverse transcribed using the Superscript kit (Invitrogen). KCNQ cDNA fragments were amplified using the Advantage GC melt kit (Clontech, Basingstoke, UK). Amplified cDNA fragments were cloned using the TOPO cloning kit (Invitrogen, Groningen, The Netherlands) and sequenced to confirm their identity.

Single-cell PCR. Single-cell PCR analysis was performed as previously described (Shah et al., 2002). Briefly, cultured neurons were collected into 7.5 μl of recording solution and eluted into an Eppendorf tube containing 2.5 μl of first-strand buffer [a 2 mM concentration of each DTP, 20 μM oligo-dT_{15}, 40 mM dithiothreitol, and 20 U of RNase inhibitor (Roche Molecular Biochemicals, Indianapolis, IN)]. Reverse transcription (RT) of mRNA transcripts was initiated by addition of 100 U of Moloney murine leukemia virus reverse transcriptase RNase H(−) point mutant (Promega, Madison, WI) followed by incubation at 37°C for 1 hr. A multiplex PCR protocol was then used to amplify cDNA for KCNQ2–5 simultaneously. Primers were designed to be intron-spanning (on the basis of human KCNQ genes) and have been described fully by Shah et al. (2002).

Immunofluorescence
DRG neurons cultured on glass coverslips were initially rinsed three times for 5 min/rinse with PBS. Cells were fixed with freshly prepared 4% paraformaldehyde for 30 min at room temperature and then quenched twice with 0.37% glycine and 0.27% ammonium chloride in PBS for 10 min. After several rinses with PBS, the cells were permeabilized with 0.1% Triton X-100 in PBS for 15 min and then incubated for 60 min in a blocking solution containing 2% bovine serum albumin (BSA) plus 2% FCS in PBS. After three rinses with 1% BSA in PBS, the cells were incubated overnight at 4°C with primary antibody diluted in 1% BSA in PBS. The primary antibodies used were goat anti-KCNQ2 (1:100; Santa Cruz Biotechnology, Santa Cruz, CA), rabbit anti-KCNQ3 (1:100; a gift from S. Burbidge, GlaxoSmithKline), goat anti-KCNQ3 (1:100; Santa Cruz Biotechnology), and rabbit anti-KCNQ5 (1:500; a gift from A.Villaroel, Instituto Cajal–Consejo Superior de Investigaciones Científicas, Madrid, Spain).

Cells were rinsed six times for 5 min/rinse with 1% BSA in PBS and then incubated with tetramethylrhadomine isothiocyanate- or FITC-coupled secondary antibodies (1:1000; Molecular Probes, Eugene, OR) for 60 min. After six additional washes with 1% BSA in PBS and a final wash with PBS alone, the coverslips were mounted on ethanol-cleaned slides using a fluorescence mounting medium (Dako, High Wycombe, UK) and visualized using a confocal microscope. Images were obtained using either a 40 or 100× objective with the sequential acquisition setting

at 1024 × 1024 pixel resolution. Control experiments in which the primary antibody was omitted or preincubated with its relevant immunogenic peptide were performed to determine antibody specificity.

In vivo *spinal cord electrophysiology*
Model of neuropathy. Male Sprague Dawley rats, initially weighing 130–150 gm, were used for *in vivo* electrophysiological studies. All experimental procedures were approved by the Home Office and followed the guidelines of the International Association for the Study of Pain (Zimmerman, 1983). The spinal nerve ligation model of neuropathic pain was performed as first described by Kim and Chung (1992). Briefly, under gaseous halothane anesthesia (3.5% for induction and 1.5% for maintenance) in N_2O and O_2 (50:50), the L5 and L6 spinal nerves were exposed as follows. The rat was placed in a prone position, and a midline incision was made from L4 to S2. A little of the left paraspinal muscles and left spinous process of the L5 lumbar vertebra were removed to expose the L4 and L5 spinal nerves. L6 was identified lying just under the sacrum. Using 6-0 silk thread, the left spinal nerves L5 and L6 were tightly ligated in the section between their dorsal root ganglion and their conjunction to form the sciatic nerve. Hemostasis was confirmed; the wound was sutured; and the animal recovered from anesthesia.

Behavioral testing. For 2 weeks after surgery, the rats were housed in groups of four in plastic cages under a 12 hr day/night cycle, and their general health was monitored. Successful reproduction of the neuropathic model was confirmed by behavioral testing (postoperative days 2, 3, 5, 7, 9, 12, and 14). Rats were placed in transparent plastic cubicles on a mesh floor, and the sensitivities of both the ipsilateral and contralateral plantar surfaces of the hindpaws to normally non-noxious punctate mechanical stimuli, using von Frey filaments (bending forces, 1, 5, and 9 gm) were assessed as described by Matthews and Dickenson (2001).

Neuronal characterization. Electrophysiology was performed 14–17 d after surgery and on nonoperated naive rats of similar size (Dickenson and Sullivan, 1986). Briefly, anesthesia was induced with 3% halothane in N_2O and O_2 (66:33); a cannula was inserted into the trachea; and the rat was secured in a stereotaxic frame. A laminectomy was performed (vertebrae L1–L3) to expose segments L4 and L5 of the spinal cord, and the level of halothane was reduced to 1.8%. Extracellular recordings of single convergent neurons, located deep within the dorsal horn (>500 μm), receiving input from the toe region ipsilateral to the spinal nerve ligation (when performed), were made using a parylene-coated tungsten electrode. Neurons selected responded to both noxious (pinch) and non-noxious (touch) stimuli. Spikes evoked by natural stimuli applied constantly over 10 sec were quantified by the application of both punctate mechanical (von Frey filaments, 9 and 75 gm) and thermal (constant water jet at 45°C) stimuli applied to the center of the receptive field of the neuron. The thermal response to 45°C was determined by subtracting the response to 32°C (a non-noxious temperature to ascertain any mechanical response evoked by the water jet) from the response to 45°C. All responses to natural stimuli were normalized by the subtraction of any spontaneous activity measured before the application of each stimulus. Response of the neuron to transcutaneous electrical stimulation was established by insertion of two fine needles into the center of its peripheral receptive field. A test consisted of a train of 16 stimuli (2-msec-wide pulse at 0.5 Hz at three times the threshold required to evoke a C fiber response), and a poststimulus histogram was constructed. Electrically evoked spikes were separated on a latency basis into Aβ fibers (0–20 msec), Aδ fibers (20–90 msec), C fibers (90–300 msec), and postdischarge spikes (300–800 msec). The "input" represents the number of spikes (90–800 msec) evoked by the first stimulus of the train. "Excess spikes" are measures of "windup," which is increased NMDA receptor-mediated neuronal excitability to repeated constant stimulation (Dickenson, 1995). Excess spikes were calculated as the total spikes (90–800 msec) after a 16-stimulus train − input × 16. Windup graphs for individual neurons show how the combined number of evoked C fiber and postdischarge action potentials (i.e., 90–800 msec) increase with each repeated electrical stimulation.

Pharmacological studies. The testing protocol, initiated every 10 min, consisted of an electrical test followed by the natural stimuli, as described. Stabilization of the neuronal responses was confirmed with at least three consistent predrug responses (<10% variation), for all measures. These values were then averaged to generate predrug control values with which to compare the effect of retigabine administration on subsequent evoked responses. Retigabine was dissolved in saline and applied directly onto the spinal cord in 50 μl volumes. Each dose (10, 30, 60, and 90 μg) was followed until maximum effects were exerted (a minimum of 60 min), when the next dose would be applied cumulatively. The results were calculated as maximum percentage of inhibition from the averaged predrug value for each neuron, and the overall results for each dose were expressed as mean ± SEM of the normalized data. Statistical analysis of maximal drug effects at each dose compared with the averaged predrug value was determined by paired *t* test on raw data. An unpaired *t* test on the normalized data was used for the comparison of drug effects between different experimental groups. The level of significance was taken as $p <$ 0.05.

Animal model of nociceptive and inflammatory hypersensitivity
The methods for induction and assessment of carrageenan-induced hyperalgesia have been described previously (Clayton et al., 2002).

Induction of carrageenan-induced hyperalgesia. Briefly, male randombred hooded rats were injected intraplantar into the left hind paw with 100 μl of 2% carrageenan. To assess the analgesic effect of retigabine and its antagonism by XE991, animals were dosed orally at 5 mg/kg with a combination of vehicle plus vehicle, vehicle plus retigabine, vehicle plus XE991, or retigabine plus XE991 2 hr after the carrageenan dose and 1 hr before assessment of hyperalgesia.

Behavioral assessment of hyperalgesia. In normal rats, body weight is distributed equally between the two hindpaws. However, body weight is redistributed when one hindpaw is inflamed or painful so that less weight is placed on the affected paw. Thus, redistribution of body weight after induction of inflammation may be used to assess the development of hyperalgesia. Weight bearing was examined using a dual-channel weight averager (Bioengineering; GlaxoSmithKline). The two hindpaws were placed on separate sensors, and the percentage of weight distribution was calculated over 7 sec (Clayton et al., 1997).

Data analysis. All data are expressed as mean ± SEM. In all experiments, there were seven animals per group. Statistical analysis was performed to compare control responses with test responses using ANOVA followed by a *post hoc* Kruskal–Wallis test on raw data. The level of significance was taken as $p < 0.05$.

Drugs and chemicals
Retigabine and XE991 (10,10-*bis* (4-pyridinyl-methyl)-9(10H)-anthracenone) were gifts from GlaxoSmithKline (Stevenage, UK) and DuPont (Wilmington, DE), respectively. Linopirdine was purchased from Research Biochemicals (Natick, MA, USA). Margatoxin (MgTX) was obtained from Peptide Institute. TEA was purchased from Lancaster Synthesis (Morecambe, UK). WAY-123,398 ([[(4-methylsulfonyl) amido]benzene-sulfonamide) was a gift from Wyeth-Ayerst Research (Princeton, NJ). Nerve growth factor was purchased from Tocris (Bristol, UK). All other drugs and chemicals were obtained from Invitrogen, Sigma (Gillingham, UK), or BDH (Poole, UK).

Results
Identification of the M current
The $I_{K(M)}$ was identified by using a standard deactivation voltage protocol, in which the cell is held at a steady depolarized potential to activate the current and then deactivated by intermittent hyperpolarizing steps (Fig. 1*A*); the contribution of $I_{K(M)}$ to the outward current is then diagnosed from the slow deactivation tail current (Fig. 1*B*) (Brown and Adams, 1980). The reason for using this protocol is that, because the M current does not inactivate, contamination by other voltage-gated currents is minimized.

An M current so defined was identified in each of 30 small neurons tested (capacitance, 20.4 ± 1.1 pF; range, 11.5–34 pF). Of 22 cells so tested, 16 also responded to 1 μM capsaicin with an inward current (204 ± 97 pA at –50 mV) and an increase in conductance (data not shown), whereas the remaining 6 of 22

cells showed no response. Capsaicin-sensitive and -inse-nsitive cells had the same size (mean capacitance, 19.9 ± 1.4 and 17.3 ± 3.3 pF, respectively; $p > 0.05$). The small size of cells expressing $I_{K(M)}$ and their sensitivity to capsaicin suggest that they were probably nociceptors.

The $I-V$ relationship for $I_{K(M)}$, computed from the initial amplitude of the de-activation tail currents (Adams et al., 1982), showed a negative threshold of activation (-60 mV), close to the resting membrane potential, and a reversal potential for its tail of approximately -80 mV, close to E_K (Fig. 1C). Deactivation of $I_{K(M)}$ was best-fitted by two exponentials, with the time constants, τ_{fast} and τ_{slow}, equal to 76.4 ± 9.9 and 583 ± 134 msec, respectively, at -50 mV ($n = 9$). These time constants were very close to τ_{fast} and τ_{slow} for $I_{K(M)}$ in rat sympathetic neurons and those for the KCNQ2 plus KCNQ3 current ($I_{KCNQ2+KCNQ3}$) in transfected CHO cells (Table 1). Deactivation showed the characteristic acceleration with increasing hyperpolarization; both τ_{fast} and τ_{slow} shortened, with τ_{fast} falling e-fold for a 52.6 mV hyperpolarization (Fig. 1D).

$I_{(K)M}$ was also detected in 9 of 10 large cells tested (capacitance, >100 pF). However, in contrast to small cells, $I_{K(M)}$ was not clearly visible in the initial macroscopic current recordings because it was masked by the presence of a large "instantaneous" outward current (I_{Ins}) and a slow hyperpolarization-activated inward current (I_h), which were activated positive and negative to V$_{rest}$, respectively (Fig. 1E). Nevertheless, the presence of $I_{(K)M}$ became apparent after inhibition of I_{Ins} and I_h with 100 nM α-dendrotoxin (α-DaTX) or 1–50 nM MgTX and 1 mM Cs$^+$, respectively (Fig. 1F, note the increased gain). Confirmation of this current as $I_{(K)M}$ was achieved using retigabine (10 μM; Fig. 1H) and XE991 (0.03–10 μM; Fig. 1I), which, as anticipated, activated and blocked the current, respectively (see below).

K$^+$ channel pharmacology
Linopirdine has previously been demonstrated to be a potent inhibitor of the M current in hippocampal and rat sympathetic neurons (Aiken et al., 1995; Lamas et al., 1997). $I_{K(M)}$ in DRG neurons showed a high sensitivity to linopirdine (Fig. 2B,C; IC$_{50}$, 2.1 ± 0.2 μM; $n = 8$) and to its analog XE991 (Fig. 2C; IC$_{50}$, 0.26 ± 0.01 μM; $n = 6$) (Wang et al., 1998), as well as to Ba^{2+} (data not shown; IC$_{50}$, 0.3 ± 0.04 mM; $n = 4$). One to 40 μM MgTX and αDaTX (blockers of slowly inactivating K$_v$1.1, 1.2, and 1.3 and 1.1, 1.2, and 1.6 channels, respectively; Kaczorowski and Garcia, 1999), 1 mM 4-AP, or 10 μM WAY-123,398 (a blocker of ether-a-go-go-related gene potassium channels, which are capable of generating M-like currents; Se-
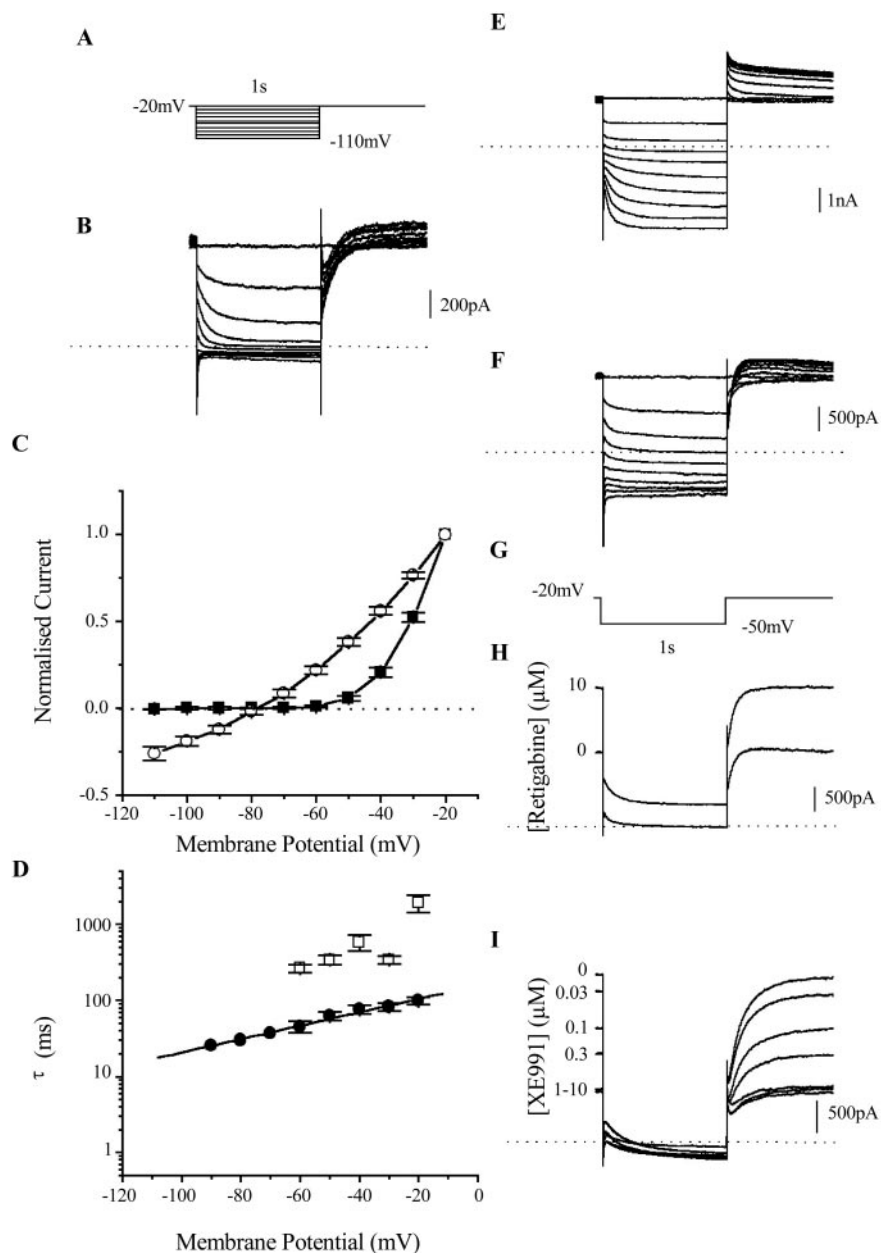

Figure 1. M currents are expressed in both small and large DRG neurons. A, Standard deactivation protocol for recording $I_{K(M)}$. B, Representative current recorded from a small (17.3 pF) DRG neuron. C, Mean instantaneous (open circles) and leak-subtracted steady-state (filled circles) $I-V$ relationships for $I_{K(M)}$ recorded from small DRG neurons ($n = 17$; capacitance, 19.4 ± 1.2pF), obtained by measuring the current at the beginning and end of the voltage pulse, respectively. Leak subtraction was performed by extrapolation of the linear portion of the $I-V$ curve negative to -70 mV. D, Semilogarithmic plot of the voltage dependence of the fast (filled circles) and slow (open squares) deactivation time constants (τ) of $I_{K(M)}$ recorded from small DRG neurons ($n = 9$; capacitance, 19.0 ± 1.2 pF). E, F, Representative current recorded from a large (>100 pF) DRG neuron before (E) and after (F) block of I_{Ins} and I_h with 100 nM α-DaTX and 1 mM Cs$^+$, respectively. Note the gain increase in F. G, Voltage protocol used for recording $I_{K(M)}$ in the absence and presence of various concentrations of K$^+$ channel blockers and M channel blockers and activators. H, I, Enhancement (H) and inhibition (I) of $I_{K(M)}$ recorded from a large DRG neuron with 10 μM retigabine and 0.03–10 μM XE991, respectively.

lyanko et al., 1999) had no effect. Thus, $I_{K(M)}$ in DRG neurons closely resembled that in sympathetic neurons and also the currents generated by its presumed KCNQ2 and KCNQ3 genes when coexpressed in *Xenopus* oocytes or mammalian cell lines (Table 2).

TEA sensitivity
KCNQ2–5 subunits vary in their sensitivity to TEA (Yang et al., 1998; Wang et al., 1998; Kubisch et al., 1999; Hadley et al., 2000;

Table 1. Kinetic components in $I_{K(M)}$ in rat DRG and SCG neurons and in $I_{KCNQ2+KCNQ3}$ in transfected CHO cells

Current	Kinetic components	
	τ_{fast} (msec)	τ_{slow} (msec)
$I_{K(M)}$ DRG ($n = 9$)	76.4 ± 9.9	583 ± 134
$I_{K(M)}$ SCG ($n = 41$)	83.9 ± 4.2	485 ± 35.9
$I_{KCNQ2+KCNQ3}$ CHO ($n = 8$)	101 ± 15	309 ± 36

$I_{K(M)}$ was recorded from rat DRG and SCG neurons, and $I_{KCNQ2+KCNQ3}$ was recorded from transfected CHO cells. $I_{KCNQ2+KCNQ3}$ was produced by cotransfecting rat KCNQ3 with fast and slow splice variants of rat KCNQ2 at a 1:1:1 cDNA ratio (Pan et al., 2001). Current deactivation was recorded in response to a voltage step to −50 mV from a holding potential of −20 mV. Means ± SEM of time constants (τ) were obtained from deactivation relaxations recorded at −50 mV. Numbers of cells are in parentheses. Data on $I_{K(M)}$ in SCG neurons and $I_{KCNQ2+KCNQ3}$ in CHO cells are from Pan et al. (2001).

Table 2. Effects of K^+ channel blockers on $I_{K(M)}$ in DRG and SCG neurons and $I_{KCNQ2+KCNQ3}$ in mammalian cells or frog oocytes

Blocker	$I_{K(M)}$		$I_{KCNQ2+KCNQ3}$
	DRG	SCG	
Linopirdine			
IC$_{50}$ (n)	2.1 ± 0.2 μM (8)	3.4 ± 0.3 μM[a]	4.0 ± 0.5 μM[b]
n_H	0.9 ± 0.08	1.13 ± 0.1	
XE991			
IC$_{50}$ (n)	0.26 ± 0.01 μM (6)	0.98 ± 0.15 μM[b]	0.6 ± 0.1 μM[b]
n_H	1.1 ± 0.06		
TEA	One-component fit		
IC$_{50}$ (n)	0.2–0.6 mM (2/7)	5.2 ± 0.5 mM (7)	3.8 ± 0.2 mM[c]
	3.9–4.7 mM (3/7)		
n_H	0.6–1.0	0.7 ± 0.05	0.8
Ba^{2+}			
IC$_{50}$ (n)	0.3 ± 0.04 mM (4)	0.4 ± 0.03 mM[d]	NT
n_H	0.7 ± 0.07	0.8 ± 0.05	

Values are mean ± SEM. Numbers of cells are in parentheses. IC$_{50}$ values and Hill coefficients (n_H) were determined from dose–response curves of the type illustrated in Figure 2. NT, Not tested.

[a]Lamas et al. (1997) (rat SCG).

[b]Wang et al. (1998) ($I_{K(M)}$, SCG neurons; $I_{KCNQ2+KCNQ3}$, frog oocytes).

[c]Hadley et al. (2000) (CHO cells).

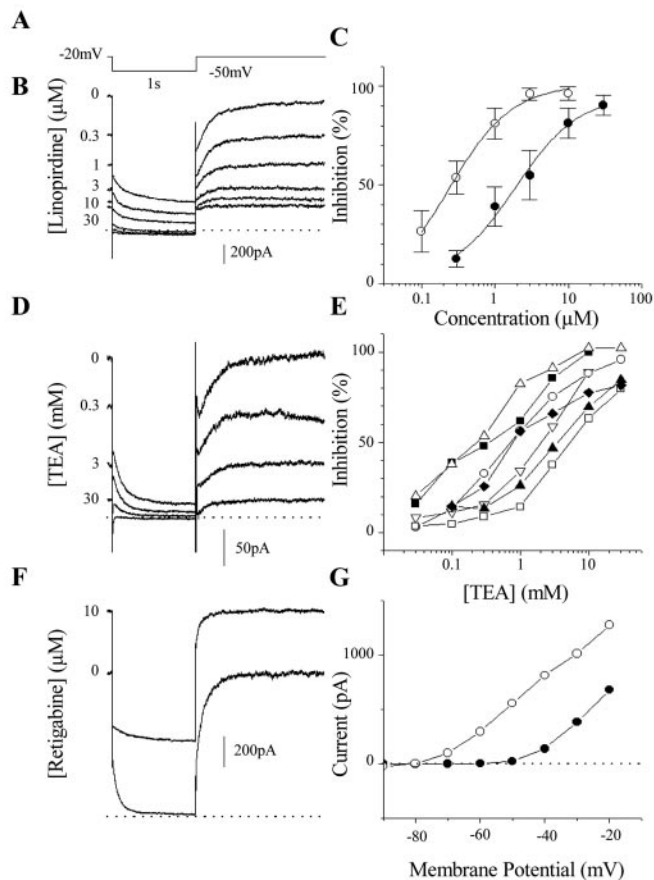[d]Selyanko et al. (1999) (mouse SCG).

Figure 2. Pharmacology of $I_{K(M)}$ in small DRG neurons. *A*, Voltage protocol used for recording $I_{K(M)}$ in the absence and presence of various concentrations of K^+ channel blockers and M channel blockers and activators. *B*, *D*, *F*, $I_{K(M)}$ recorded in response to various concentrations of linopirdine (*B*), TEA (*D*), and retigabine (*F*). *C*, concentration dependence of inhibition of $I_{K(M)}$ by linopirdine (closed circles) and XE991 (open circles). *E*, Concentration dependence of inhibition of $I_{K(M)}$ by TEA in individual DRG neurons. *G*, Steady-state *I–V* relationship under control conditions (filled circles) and in the presence of 10 μM retigabine (open circles).

Lerche et al., 2000; Schroeder et al., 2000), with KCNQ2 having the highest affinity arising from the presence of a tyrosine just downstream of the GYG pore sequence (Hadley et al., 2000). When measured in individual DRG neurons, the TEA sensitivity was variable (Fig. 2*D*,*E*), indicating different proportions of TEA-sensitive and -insensitive subunits. Thus, in some cells (two of seven), the TEA sensitivity was very high (IC$_{50}$, ∼0.2–0.6 mM), suggesting expression of KCNQ2 subunits only, whereas in other cells (three of seven), the TEA sensitivity was intermediate and similar to that expected for KCNQ2/3 heteromers (IC$_{50}$, ∼3.9–4.7 mM). Two of seven cells displayed biphasic inhibition by TEA,

and a two-component Hill equation gave an improved fit (lower IC$_{50}$ values, 0.26 and 0.41 mM, upper IC$_{50}$ values, 8.55 and 3.28 mM), suggesting expression of a mixture of homomeric and heteromeric subunits.

Activation by retigabine

In seven of seven cells tested, the neuronal KCNQ channel opener retigabine (see Introduction) enhanced $I_{K(M)}$ (Fig. 2*F*) and produced a characteristic slowing of its deactivation, consistent with the negative shift in activation of neuronal KCNQ channels (Main et al., 2000; Rundfeldt and Netzer, 2000; Wickenden et al., 2000; Tatulian et al., 2001). The effect of retigabine was concentration- and voltage-dependent, being stronger at −20 than at −50 mV. Steady-state *I–V* relationships constructed in the presence and absence of retigabine showed that this outward current was reduced by membrane hyperpolarization and dissipated at approximately −80 mV, close to E_K (e.g., see Fig. 2*G*). This was accompanied by a negative shift (by 12.3 ± 3.3 mV) in zero current (resting) potential.

M current modulation and cell excitability

M current can act as a brake on repetitive firing in neurons (Brown, 1988). Thus, M channel blockers enhance repetitive firing in sympathetic (Wang et al., 1998) and hippocampal (Aiken et al., 1995) neurons. We therefore tested what effect linopirdine and retigabine might have on the firing properties of small DRG neurons during long (1 sec) depolarizing current pulses. The resting potential was close to −55 mV and was maintained at this level, if necessary, by injecting DC current. The cells were highly refractory and fired only once in response to currents of 150–200 pA or more (Fig. 3*A*). In five of five neurons, the inhibition of the M current by 30 μM linopirdine reduced the threshold of firing, and in two of them, it produced a brief burst of multiple firing (Fig. 3*B*).

In contrast, retigabine (10 μM) hyperpolarized the membrane and increased the threshold of firing (Fig. 3*D*). When the membrane potential was restored to the initial level by injecting the depolarizing DC current, the voltage changes associated with current pulses were much smaller than in the control, implying an increase in membrane conductance (Fig. 3*E*). The increase in
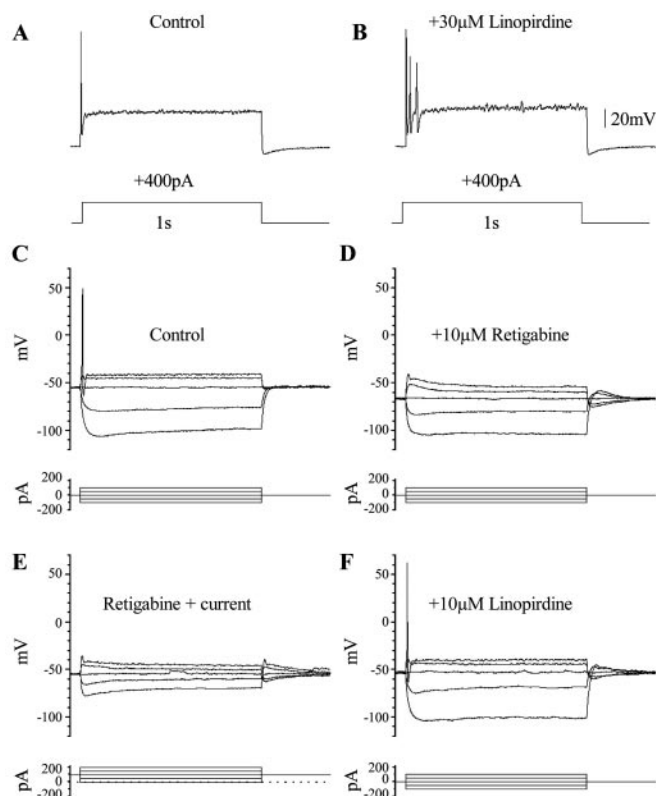
Figure 3. Modulation of excitability in small DRG neurons by inhibiting $I_{K(M)}$ with linopirdine and by activating $I_{K(M)}$ with retigabine. *A*, Single firing was produced by a 400 pA depolarizing current pulse in the control, whereas two or three spikes were produced in response to the same current injection in the presence of 30 μM linopirdine (*B*). *C*, Under control conditions, electrotonic potentials and a single action potential (top) were produced by hyperpolarizing and depolarizing current pulses (bottom), respectively. *D*, Ten micromolar retigabine hyperpolarized the membrane by 12 mV and abolished the spike. *E*, A depolarizing current injection restores the membrane potential to the initial value in presence of 10 μM retigabine. The action potential remains absent and reduced voltage responses are produced, owing to an enhanced membrane conductance. *F*, The effects of retigabine on spike initiation and membrane conductance were reversed by 10 μM linopirdine. The data in panels *A* and *B* and *C–F* were obtained from two different cells.

Figure 4. KCNQ subunit mRNA expression in rat dorsal root ganglion neurons. *A*, Reverse transcription-PCR analysis of RNA isolated from adult rat DRG using primer pairs for KCNQ subunits 2–5. *B*, Single cell PCR analyses on cultured rat DRG small and large neurons using primer pairs for KCNQ subunits 2–5. Arrows point to KCNQ subunit-specific PCR products. Control reactions were performed using primer pairs on plasmid constructs containing the coding sequence for each of the KCNQ subunits 2–5. PCR products were separated by electrophoresis through 2% Metaphor agarose (FMC Bioproducts, Rockland, MD) and a 1 kb plus DNA ladder (Invitrogen).

conductance and inhibition of firing produced by retigabine could then be reversed by adding 10 μM linopirdine (Fig. 3*F*). Similar effects of retigabine were obtained from five other cells; in two of two cells tested, the effect of retigabine was reversed by 10 μM XE991.

Expression of KCNQ subtypes in DRG neurons
RT-PCR and single-cell PCR analyses were used to determine the expression of the family of KCNQ genes in rat DRG. KCNQ2–5 but not KCNQ1 were expressed at detectable levels in whole rat DRG (Fig. 4*A*). Several controls to support our observations are included. First, no amplified bands were detected in the absence of reverse transcriptase (second lane), thus confirming that the amplified bands were of cDNA and not genomic origins. Second, each of the amplified fragments was cloned and sequenced to confirm its identity. Thirdly, either brain (third lane) or heart tissue (fifth lane) was used as a positive control, allowing confirmation of a negative signal in the DRG. These results confirm that all of the potential molecular correlates of $I_{K(M)}$ are expressed in the DRG. A low level of KCNQ1 expression in the brain was also detected, as previously reported (Kubisch et al., 1999). Interestingly, KCNQ4 and low levels of KCNQ5 expression were also
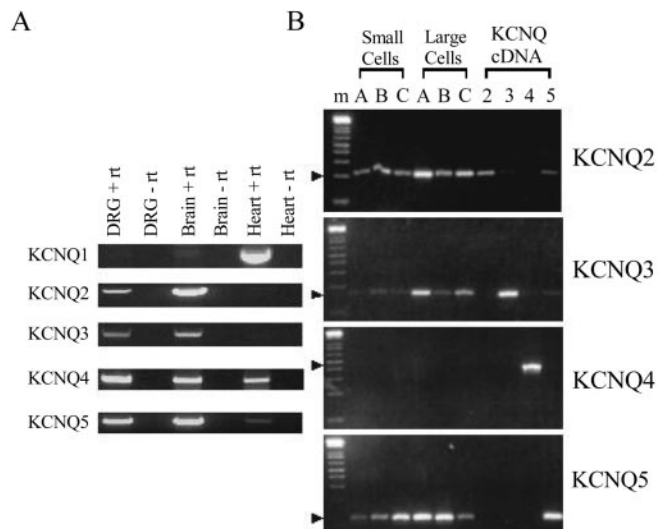
detected in the heart (Fig. 4*A*, fifth lane). In the case of KCNQ4, this confirms previous data from Northern analysis (S. A. Burbidge, D. Crowther, and P. Sanseau, personal communication).

Single-cell PCR was used to determine the KCNQ subunit expression in individual small and large neurons when cultured as for the electrophysiological experiments (Fig. 4*B*). PCR products of the predicted size from cDNA were obtained for KCNQ2, KCNQ3, and KCNQ5 from both small and large DRG neurons (*n* = 12). Neurons isolated from both acutely dissociated cultures and 3 d primary cultures gave identical results. KCNQ4 mRNA was not detected in either small or large DRG neurons, indicating that its expression in whole ganglia (Fig. 4*A*) refers to other cell types within the ganglia. Control reactions performed in parallel using plasmid DNA containing the coding sequence for KCNQ2–5 gave specific PCR products for each primer pair. Contamination by genomic DNA can be excluded because the primer pairs were intron spanning and because longer PCR products were not evident in the single cell PCRs.

Immunofluorescence results
Confocal immunofluorescence microscopy of cultured DRG neurons revealed variable expression of KCNQ2, 3 and 5 immunoreactivity on the somata and neuronal processes of both small and large neurons (Fig. 5). Thus, although some cells expressed both KCNQ2 and KCNQ3, others expressed KCNQ2 in the absence of KCNQ3 (Fig. 5*C*). Likewise, although some cells expressed both KCNQ3 and KCNQ5, others expressed KCNQ3 in the absence of KCNQ5 (Fig. 5*I*). Colocalization of KCNQ2 and KCNQ5 (Fig. 5*F*) was also detected, although it is likely that such cells also express KCNQ3 because KCNQ2 and KCNQ5 do not form heteromeric channels (Lerche et al., 2000; Schroeder et al., 2000). Costaining for KCNQ2, 3, and 5 subunits could not be performed because of species limitations of the secondary antibodies.
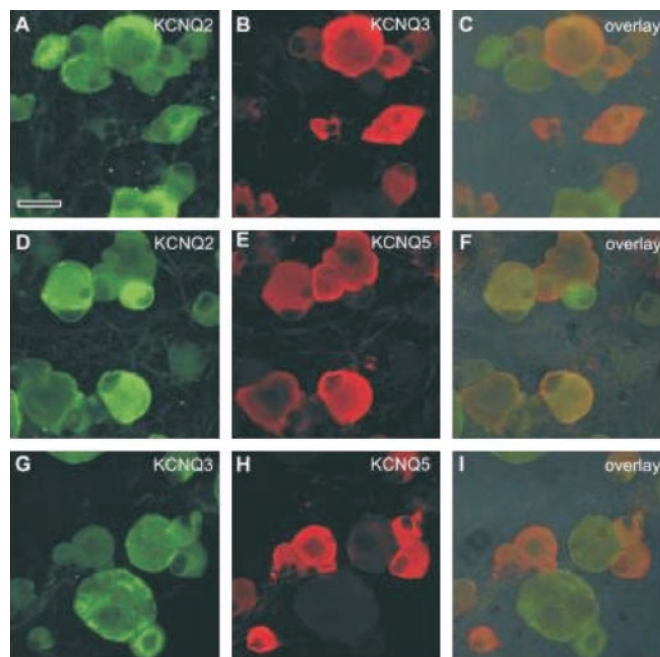
Figure 5. Immunocytochemistry with antibodies to KCNQ2, KCNQ3, and KCNQ5 reveals variable expression of KCNQ subunits in small and large DRG neurons. Confocal images of KCNQ2, KCNQ3, and KCNQ5 immunostaining in cultured DRG neurons are shown. *A, B, D, E, G, H*, Immunostaining images for individual antibodies. *C, F, I*, Overlays of immunostaining for KCNQ2 and KCNQ3 (*C*), KCNQ2 and KCNQ5 (*F*), and KCNQ3 and KCNQ5 (*I*). Scale bar, 25 μm.

In vivo spinal cord electrophysiology and pharmacology in a model of neuropathy
Rats subjected to spinal nerve ligation (see Materials and Methods) exhibited abnormal foot posture ipsilateral to nerve injury, whereby toes were held together in a "guarding" behavior. Successful replication of the nerve injury model was confirmed by the development of mechanical allodynia in the injured hindpaw, displayed as a brisk withdrawal, in some cases accompanied by shaking and licking of the foot, to normally innocuous von Frey filaments (1, 5, and 9 gm bending forces). Increased frequency of foot withdrawal was observed with increased bending force. Mechanical allodynia was evident at postoperative day 2, reached a maximum at days 7–12, and was still present at day 14 (Matthews and Dickenson, 2001). Consistent withdrawal responses were never exhibited by the contralateral hindpaw.

Recordings were obtained from ipsilateral dorsal horn neurons in 10 animals after spinal nerve ligation and in 11 naive animals. No significant differences were found between the two experimental groups in the mean values of recorded neuron depth and the responses evoked by electrical and natural stimulation. However, neurons of spinal nerve-ligated animals showed appreciable ongoing spontaneous activity (mean rate, 2.75 ± 1.09 Hz), whereas no such activity was observed in naive animals; this difference was significant ($p < 0.02$).

Application of retigabine (10–90 μg) produced statistically significant dose-related inhibitions of both the electrically and naturally evoked neuronal responses from the determined predrug control values in both experimental groups (Fig. 6; $p < 0.05$; $n = 5$–10). Clear effects were seen at ~60 min after application of the drug (Fig. 6*I*). In naive and nerve-injured rats, the Aβ fiber response was least affected by spinal retigabine, with mean maximal inhibitions from predrug control values at the top dose only reaching 23 ± 3 and $33 \pm 8\%$, respectively (Fig. 6*C*). The other electrically evoked neuronal responses were more susceptible to

the inhibitory actions of retigabine. Thus, in nerve-injured animals, the C fiber, Aδ fiber, and input responses reached similar mean maximal observed inhibitions in the range of 61 ± 4 to $73 \pm 9\%$ (Fig. 6*A,B*, respectively). Greater inhibitory effects of the high dose of retigabine were observed on the postdischarge and excess spike measurements (Fig. 6*D,E*, respectively), such that, at 90 μg, retigabine maximally inhibited both measures in ligated animals by $81 \pm 5\%$, whereas in naive rats, the effect was 69 ± 11 and $65 \pm 7\%$ from predrug control values for postdischarge and excess spikes, respectively. This is further emphasized by the examples in Figure 6, *G* and *H*, in which windup (the increase in the number of spikes per stimulus over the train of electrical impulses, which generates the postdischarge and excess spikes; Dickenson, 1995) is clearly reduced more after nerve injury, as shown by the flattening of the windup slope. Overall, there was no difference in the predrug values of these measures of neuronal excitability for the naive and nerve-injured groups.

Retigabine (90 μg) also inhibited the naturally evoked neuronal responses to innocuous (von Frey, 9 gm) and noxious (von Frey, 75 gm) punctate mechanical stimuli and noxious heat (45°C) in both experimental groups by amounts within the range of 65 ± 13 to $87 \pm 5\%$ from the predrug control (data not shown).

Analgesic properties of retigabine
To assess the analgesic effect of retigabine, we used a model for chronic pain in which the irritant carrageenan is injected into one hindpaw. This leads the animal to distribute its weight unevenly between the two legs. Thus, 3 hr after intraplantar administration of carrageenan (2%, 100 μl), there was a substantial and significant decrease in the weight bearing on the left hindpaw, such that animals distributed only $21 \pm 3\%$ of their hind leg load onto the inflamed paw (Fig. 7), compared with the normal 50% after injection of vehicle alone. Retigabine [5 mg/kg, orally (p.o.)] strongly reduced this asymmetry, so that the weight borne on the inflamed leg increased to $41 \pm 2\%$. This effect was antagonized by coadministration of XE991 (5 mg/kg, p.o.), resulting in a weight distribution ($28 \pm 3\%$) similar to that in animals treated with vehicle alone. Interestingly, XE991 itself had no effect on weight distribution.

Discussion
In this work we have established that the sensory neurons of rat dorsal root ganglia express the KCNQ molecular substrates of neural M channels and possess identifiable M currents. We have also shown that these play a significant role in regulating the excitability of small-diameter, predominantly nociceptive neurons. As a result, the enhancement of the M current by retigabine strongly and selectively reduces responses of nociceptive neurons in the dorsal horn, an effect that is maintained after nerve injury, and exerts an analgesic action in an animal model of inflammatory pain.

Biophysically and pharmacologically, the M current that we have identified in these sensory neurons closely matched that previously reported in rat sympathetic neurons (Tables 1, 2) (Lamas et al., 1997; Wang et al., 1998; Selyanko et al., 1999; Pan et al., 2001). It also showed a good match against currents generated on coexpressing KCNQ2 and KCNQ3 cDNAs, the proposed molecular subunits of the native ganglionic M channel (Wang et al., 1998) (cf. Hadley et al., 2000; Pan et al., 2001). In fact, individual DRG neurons variably expressed three subunits from this family (KCNQ2, 3, and 5), as judged from single-cell PCR and immunocytochemical observations, and some neurons, at least,

contained mRNA for all three. This is probably true for subunit protein expression as well, to judge from the high frequency with which cells expressed immunoreactivity for each of the subunits. Karchewski et al. (2001) have also briefly reported the presence of KCNQ mRNA and protein in rat DRG neurons, with some differential subunit expression in different subpopulations.

Expression studies indicate that KCNQ2 and KCNQ3 subunits are more efficiently translated into functional membrane channels as heteromultimers than as homomultimers (Schwake et al., 2000; Selyanko et al., 2000), and the same is probably true for KCNQ3/5 heteromultimers (Schroeder et al., 2000). On the other hand, the immunocytochemistry also suggested that a proportion of neurons expressed KCNQ2 protein in the absence of KCNQ3 and hence might well carry currents through homomeric KCNQ2 channels. Support for this is provided by the high sensitivity to TEA of M currents recorded in a proportion of cells, in which the IC_{50} values (0.2–0.6 mM) approximated those obtained against homomeric KCNQ2 currents (between 0.1 and 0.4 mM; Wang et al., 1998; Hadley et al., 2000; Shapiro et al., 2000; Wickenden et al., 2000); other cells yielded IC_{50} values ~10 times greater and more in accord with the expression of KCNQ2/3 heteromultimers. A rather similar situation has been noted in sympathetic neurons isolated from rats of this (17 d) age, in which a proportion of the current was sufficiently sensitive to TEA to suggest that it was carried by homomeric KCNQ2 channels (Hadley et al., 2003). In contrast, blocking of sympathetic neuron currents in postnatal day 45 rats by TEA more closely accorded with a uniform population of heteromeric KCNQ2/3 channels. This was attributed to the incremental expression of KCNQ3 during postnatal development (Tinel et al., 1998; Hadley et al., 2003).

Many cells also expressed both KCNQ5 mRNA and KCNQ5 protein, and KCNQ3 and KCNQ5 were clearly colocalized in some cells. KCNQ5 (like KCNQ3) is very insensitive to TEA (IC_{50}, ~71 mM; Schroeder et al., 2000), so a contribution of currents through KCNQ3/5 channels should be revealed as a component of current that is not inhibited by 10–30 mM TEA (as in some hippocampal pyramidal cells; Shah et al., 2002). In practice, between 80 and 100% of the M current in small sensory neurons was inhibited at 30 mM TEA, suggesting that KCNQ3/5 channels contribute very little to the macroscopic somatic current. Again, this resembles the situation in sympathetic neurons, which also express all three subunits (KCNQ2, 3, and 5; Hadley et al., 2003). The reason for the unexpectedly small contribution of KCNQ5 or KCNQ3/5 channels to the somatic currents is not yet clear.

Because the majority of small neurons that exhibited macroscopic M currents were also activated by capsaicin, M currents were clearly strongly expressed in nociceptive neurons. However,
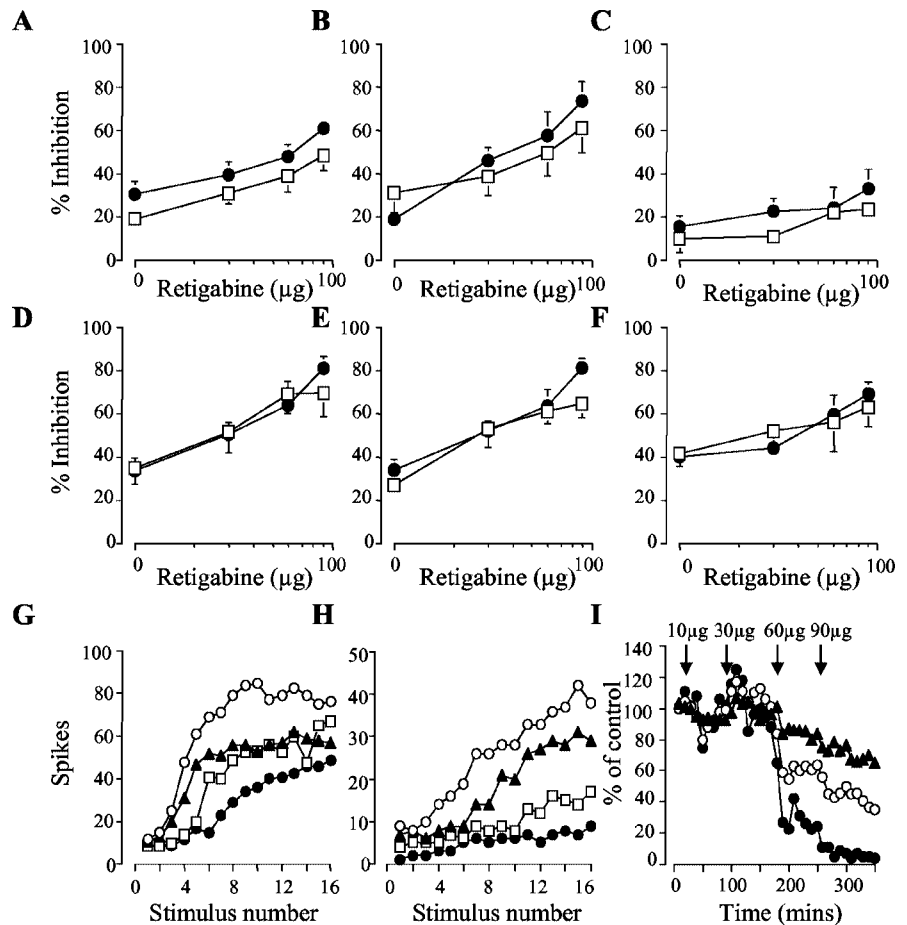

Figure 6. Effect of retigabine on electrically evoked dorsal horn responses. *A–F*, Effect of spinally applied retigabine on the electrically evoked dorsal horn neuronal responses recorded from naive (open squares; *n* = 5–10) and spinal nerve-ligated (filled circles; *n* = 5–8) rats at postoperative days 14–17. Data are expressed as maximal mean percent inhibition of the predrug values ± SEM. *A*, C fiber responses; *B*, Aδ fiber responses; *C*, Aβ fiber responses; *D*, after discharge; *E*, excess spikes; *F*, input. *G*, *H*, Inhibitory effect of spinally applied retigabine (open circle, control; filled triangle, 10 µg of retigabine; open square, 30 µg of retigabine; filled circle, 90 µg of retigabine) on individual neurons exhibiting windup recorded from naive (*G*) and spinal nerve-ligated (*H*) rats. *I*, Time course of the effect of increasing doses of spinally applied retigabine on the evoked response of a typical dorsal horn neuron recorded from a spinal nerve-ligated rat. Examples of the effect on the Aβ fiber (filled triangle), C fiber (open circle), and postdischarge (filled circle) measurements are shown with the cumulative dose indicated, and the data are expressed as percent of the predrug control value.

they were by no means exclusive to VR1 heat-sensitive nociceptive neurons; some small cells with M currents did not respond to capsaicin, and KCNQ subunits were clearly expressed in both small and large (non-nociceptive) neurons. However, in the latter cells, M currents contributed only a minor component to the subthreshold currents, which were dominated by a larger dendrotoxin-sensitive K^+ current and by the hyperpolarization-activated I_h current. In such cells, the dendrotoxin-sensitive current is likely to play the major role in determining excitability and firing behavior (Stansfeld et al., 1986), with the M current playing (at most) a subsidiary role. In contrast, but as in sympathetic neurons, the M current is the dominant subthreshold current in small sensory neurons and, as a consequence, exerts a significant effect on their excitability. Thus, inhibition of $I_{K(M)}$ with linopirdine or XE991 reduced the threshold for spike generation and favored the generation of repetitive bursts of action potentials during sustained depolarization. On the other hand, enhancement of $I_{K(M)}$ increased resting input conductance, hyperpolarized the neurons, and prevented spike generation. The increased resting conductance and hyperpolarization results from a hyper-
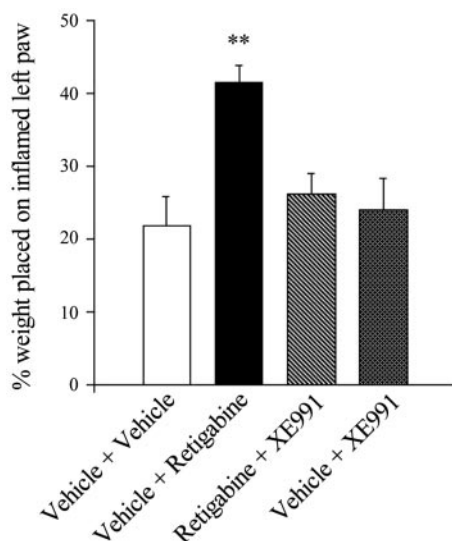
Figure 7. Analgesic activity of retigabine and block by XE991: effect of M channel activators and blockers on weight bearing in a behavioral model of inflammatory pain. Retigabine (5 mg/kg, p.o.), administered 2 hr after intraplantar carrageenan, significantly increased the weight placed on the inflamed paw. Coadministration of XE991 (5 mg/kg, p.o.) reversed the analgesic effects of retigabine, whereas treatment with XE991 (5 mg/kg, p.o.) alone had no effect on weight distribution. Bars indicate mean $\pm$ SEM of seven animals in each case. **$p <$ 0.05.

polarizing shift of the M current I–V curve, such that $I_{K(M)}$ becomes strongly activated at V_{rest} (see Tatulian et al., 2001).

Matching changes in the transmission of sensory information on application of retigabine were obtained on recording from spinal dorsal horn neurons. In agreement with the observations on sensory neuron somata, nociceptive C fiber-evoked responses were more susceptible than Aβ fiber responses. Furthermore, retigabine exerted a strong depressant effect on the delayed sensitization of dorsal horn neurons reflected in the recordings of windup. These effects might be explained most plausibly by the idea that the KCNQ/M channels identified in sensory neuron somata are also expressed on nociceptive afferent terminals, such that the enhanced M current shunts the invading action potentials and thereby reduces evoked transmitter release. There is, as yet, no direct evidence for this, but the immunofluorescence of cultured neurons indicated that KCNQ subunits are transported along neuronal processes.

Retigabine reduced C and Aδ fiber and windup responses as well as natural mechanical and thermal responses likely to correspond to Aδ and C fiber-evoked activity. The natural responses could relate to the allodynia and hyperalgesia seen after neuropathy. Overall, retigabine was as effective in reducing nociceptive dorsal horn responses after spinal nerve ligation as in the naive animals, suggesting that higher doses may be more effective. One possible explanation for this is that the density of KCNQ subunits might be enhanced after nerve injury. In partial agreement with this hypothesis, some preliminary evidence for an upregulation of KCNQ2/3 subunit proteins in L4/5 dorsal root ganglia 6–8 d after afferent nerve lesion has recently been reported (Wickenden et al., 2002). The maintained inhibitory effect of the drug after nerve injury deserves comment. The issue is that neuropathic pain is often refractory to conventional analgesics; for example, morphine is not as effective after nerve injury (Suzuki et al., 2002). Thus it is very important to note that the effects of retigabine are preserved, making these channels an attractive target for the treatment of nerve injury pain.

Finally, retigabine effectively and substantially reduced the behavioral manifestation of nociceptive activity in a model of inflammatory pain. This can unequivocally be attributed to M current enhancement because it was prevented by coadministration of the M channel blocker XE991. This accords with the recent observations of Blackburn-Munro and Jensen (2003) and suggests that enhancement of KCNQ/M channel activity might provide a novel approach to the treatment of neuropathic and other pain states.

References

Adams PR, Brown DA, Constanti A (1982) M-currents and other potassium currents in bullfrog sympathetic neurones. J Physiol (Lond) 330:537–572.
Aiken SP, Lampe BJ, Murphy PA, Brown BS (1995) Reduction of spike frequency adaptation and blockade of M-current in rat CA1 pyramidal neurones by linopirdine (Du 996), a neurotransmitter release enhancer. Br J Pharmacol 115:1163–1168.
Blackburn-Munro G, Jensen BS (2003) The anticonvulsant retigabine attenuates nociceptive behaviours in rat models of persistent and neuropathic pain. Eur J Pharmacol 460:109–116.
Boettger MK, Till S, Chen MX, Anand U, Otto WR, Plumpton C, Trezise DJ, Tate SJ, Bountra C, Coward K, Birch R, Anand P (2002) Calcium-activated potassium channel SK1- and IK1-like immunoreactivity in injured human sensory neurones and its regulation by neurotrophic factors. Brain 125:252–263.
Brown DA (1988) M-currents. In: Ion channels, Vol 1 (Narahashi T, ed), pp 55–94. New York: Plenum.
Brown DA, Adams PR (1980) Muscarinic suppression of a novel voltage-sensitive K+ current in a vertebrate neurone. Nature 283:673–676.
Clayton NM, Oakley I, Thompson S, Wheeldon A, Sargent B, Bountra C (1997) Validation of the dual channel weight averager as an instrument for the measurement of inflammatory pain. Br J Pharmacol 120:219P.
Clayton N, Marshall FH, Bountra C, O'Shaughnessy CT (2002) CB1 and CB2 cannabinoid receptors are implicated in inflammatory pain. Pain 96:253–260.
Dickenson AH (1995) Spinal cord pharmacology of pain. Br J Anaesth 75:193–200.
Dickenson AH, Sullivan AF (1986) Electrophysiological studies on the effects of intrathecal morphine on nociceptive neurones in the rat dorsal horn. Pain 24:211–222.
Hadley JK, Noda M, Selyanko AA, Wood IC, Abogadie FC, Brown DA (2000) Differential tetraethylammonium sensitivity of KCNQ1–4 potassium channels. Br J Pharmacol 129:413–415.
Hadley JK, Passmore GM, Tatulian L, Al-Qatari M, Ye F, Wickenden AD, Brown DA (2003) Stoichiometry of expressed KCNQ2/KCNQ3 channels and subunit composition of native ganglionic M-currents deduced from block by tetraethylammonium (TEA). J Neurosci 23:5012–5019.
Hunt SP, Mantyh PW (2001) The molecular dynamics of pain control. Nat Rev Neurosci 2:83–91.
Ishikawa K, Tanaka M, Black JA, Waxman SG (1999) Changes in expression of voltage-gated potassium channels in dorsal root ganglion neurons following axotomy. Muscle Nerve 22:502–507.
Jensen TS, Gottrup H, Kasch H, Nikolajsen L, Terkelsen AJ, Witting N (2001) Has basic research contributed to chronic pain treatment? Acta Anaesthesiol Scand 45:1128–1135.
Jentsch TJ (2000) Neuronal KCNQ potassium channels: physiology and role in disease. Nat Rev Neurosci 1:21–30.
Kaczorowski GJ, Garcia ML (1999) Pharmacology of voltage-gated and calcium-activated potassium channels. Curr Opin Chem Biol 3:448–458.
Karchewski L, Burbidge SA, Woolf CJ (2001) Localization of KCNQ potassium channels in primary sensory neurons. Soc Neurosci Abstr 27:2167.
Kim SH, Chung JM (1992) An experimental model for peripheral neuropathy produced by segmental spinal nerve ligation in the rat. Pain 50:355–363.
Kubisch C, Schroeder BC, Friedrich T, Lutjohann B, El-Amraoui A, Marlin S, Petit C, Jentsch TJ (1999) KCNQ4, a novel potassium channel expressed in sensory outer hair cells, is mutated in dominant deafness. Cell 96:437–446.
Lamas JA, Selyanko AA, Brown DA (1997) Effects of a cognition-enhancer, linopirdine (DuP 996), on M-type potassium currents ($I_{K(M)}$) and some

other voltage- and ligand-gated membrane currents in rat sympathetic neurons. Eur J Neurosci 9:605–616.

Lerche C, Scherer CR, Seebohm G, Derst C, Wei AD, Busch AE, Steinmeyer K (2000) Molecular cloning and functional expression of KCNQ5, a potassium channel subunit that may contribute to neuronal M-current diversity. J Biol Chem 275:22395–22400.

Main MJ, Cryan JE, Dupere JRB, Cox B, Clare JJ, Burbidge SA (2000) Modulation of KCNQ2/3 potassium channels by the novel anticonvulsant retigabine. Mol Pharmacol 58:253–262.

Marrion NV (1997) Control of M-current. Annu Rev Physiol 59:483–504.

Matthews EA, Dickenson AH (2001) Effects of spinally delivered N- and P-type voltage-dependent calcium channel antagonists on dorsal horn neuronal responses in a rat model of neuropathy. Pain 92:235–246.

McCleskey EW, Gold MS (1999) Ion channels of nociception. Annu Rev Physiol 61:835–856.

Owen DG, Marsh SJ, Brown DA (1990) M-current noise and putative M-channels in cultured rat sympathetic ganglion cells. J Physiol (Lond) 431:269–290.

Pan Z, Selyanko AA, Hadley JK, Brown DA, Dixon JE, McKinnon D (2001) Alternative splicing of KCNQ2 potassium channel transcripts contributes to the functional diversity of M-currents. J Physiol (Lond) 531:347–358.

Rae J, Cooper K, Gates P, Watsky M (1991) Low access resistance perforated patch recordings using amphotericin B. J Neurosci Methods 37:15–26.

Rundfeldt C, Netzer R (2000) The novel anticonvulsant retigabine activates M-currents in Chinese hamster ovary-cells transfected with human KCNQ2/3 subunits. Neurosci Lett 282:73–76.

Schroeder BC, Hechenberger M, Weinreich F, Kubisch C, Jentsch TJ (2000) KCNQ5, a novel potassium channel broadly expressed in brain, mediates M-type currents. J Biol Chem 275:24089–24095.

Schwake M, Pusch M, Kharkovets T, Jentsch TJ (2000) Surface expression and single channel properties of KCNQ2/KCNQ3, M-type K$^+$ channels involved in epilepsy. J Biol Chem 275:13343–13348.

Selyanko AA, Hadley JK, Wood IC, Abogadie FC, Delmas P, Buckley NJ, London B, Brown DA (1999) Two types of K$^+$ channel subunit, Erg1 and KCNQ2/3, contribute to the M-like current in a mammalian neuronal cell. J Neurosci 19:7742–7756.

Selyanko AA, Hadley JK, Wood IC, Abogadie FC, Jentsch TJ, Brown DA (2000) Inhibition of KCNQ1–4 potassium channels expressed in mammalian cells via M$_1$ muscarinic acetylcholine receptors. J Physiol (Lond) 522 3:349–355.

Selyanko AA, Passmore GM, Brown TA, Burbidge SA, Main M, Brown DA (2001) Identification and nociceptive significance of M current in small dorsal root ganglion neurons. Soc Neurosci Abstr 27:711.

Shah MM, Mistry M, Marsh SJ, Brown DA, Delmas P (2002) Molecular correlates of the M-current in cultured rat hippocampal neurons. J Physiol (Lond) 544.1:29–37.

Shapiro MS, Roche JP, Kaftan EJ, Cruzblanca H, Mackie K, Hille B (2000) Reconstitution of muscarinic modulation of the KCNQ2/KCNQ3 K$^+$ channels that underlie the neuronal M current. J Neurosci 20:1710–1721.

Stansfeld CE, Marsh SJ, Halliwell JV, Brown DA (1986) 4-Aminopyridine and dendrotoxin induce repetitive firing in rat visceral sensory neurones by blocking a slowly inactivating outward current. Neurosci Lett 64:299–304.

Suzuki R, Dickenson AH (2000) Neuropathic pain: nerves bursting with excitement. NeuroReport 11:R17–R21.

Suzuki R, Matthews EA, Dickenson AH (2002) Neurobiology of neuropathic pain: mode of action of anticonvulsants. Eur J Pain 6:51–60.

Tatulian L, Delmas P, Abogadie FC, Brown DA (2001) Activation of expressed KCNQ potassium currents and native neuronal M-type potassium currents by the anti-convulsant drug retigabine. J Neurosci 21:5535–5545.

Tinel N, Lauritzen I, Chouabe C, Lazdunski M, Borsotto M (1998) The KNCQ2 potassium channel: splice variants, functional and developmental expression. Brain localization and comparison with KCNQ3. FEBS Lett 438:171–176.

Tokimasa T, Akasu T (1990) ATP regulates muscarine-sensitive potassium current in dissociated bull-frog primary afferent neurones. J Physiol (Lond) 426:241–264.

Wang HS, Pan Z, Shi W, Brown BS, Wymore RS, Cohen IS, Dixon JE, McKinnon D (1998) KCNQ2 and KCNQ3 potassium channel subunits: molecular correlates of the M-channel. Science 282:1890–1893.

Watanabe H, Nagata E, Kosakai A, Nakamura M, Yokoyama M, Tanaka K, Sasai H (2000) Disruption of the epilepsy KCNQ2 gene results in neural hyperexcitability. J Neurochem 75:28–33.

Waxman SG, Dib-Haji S, Cummins TR, Black JA (1999) Sodium channels and pain. Proc Natl Acad Sci USA 96:7635–7639.

Wickenden AD, Yu W, Zou A, Jegla T, Wagoner PK (2000) Retigabine, a novel anti-convulsant, enhances activation of KCNQ2/Q3 potassium channels. Mol Pharmacol 58:591–600.

Wickenden AD, Ye F, Liu Y, McNaughton-Smith G, Roeloffs R, Rigdon GC (2002) KCNQ channel expression in rat DRG following nerve ligation. Soc Neurosci Abstr 454.7.

Yang WP, Levesque PC, Little WA, Conder ML, Ramakrishnan P, Neubauer MG, Blanar MA (1998) Functional expression of two KvLQT1-related potassium channels responsible for an inherited idiopathic epilepsy. J Biol Chem 273:19419–19423.

Zimmerman M (1983) Ethical guidelines for investigations of experimental pain in conscious animals. Pain 16:109–110.